P3.17

RETRIEVING SURFACE DOWNWELLING LONGWAVE RADIATION FROM SATELLITE MEASUREMENTS: IMPROVEMENT OF THE ZHOU-CESS ALGORITHM

Yaping Zhou[1], David P. Kratz[2], Anne C. Wilber[3], Shashi K.Gupta[3] and Robert D. Cess[4]

[1]Goddard Earth Sciences & Technology Center, University of Maryland Baltimore County, Greenbelt, MD
[2]Climate Science Branch, NASA Langley Research Center, Hampton, VA
[3]Analytical Services & Materials, Inc., Hampton, VA
[4] Marine Sciences Research Center, Stony Brook University, Stony Brook, NY

1. INTRODUCTION

Using detailed studies based upon radiative transfer model calculations and surface radiometric measurements, Zhou and Cess (2001) formulated algorithm development strategies for retrieving surface downwelling longwave radiation (SDLW). Their studies demonstrated that clear sky SDLW could be largely determined by surface upwelling longwave flux and column precipitable water vapor. For cloudy sky cases, they used cloud liquid water path as an additional parameter to account for the effects of clouds. An illustrative algorithm was derived and tested using observational data from Atmospheric Radiation Measurements (ARM) Program (Stokes and Schwartz 1994) measurements at the U.S. Southern Great Plain (SGP) and Tropical Western Pacific (TWP) sites.

Since the algorithm was derived and tested for mid-latitude and tropical conditions, there was concern that the algorithm might not perform well for extremely cold and dry conditions. Indeed, once data had become available from the ARM North Slope of Alaska (NSA) (Stamnes et al., 1999), we found large biases when the algorithm was applied to surface measurements from that location. Sensitivity studies demonstrated that the algorithm significantly underestimates SDLW when atmospheric water vapor is low. Meanwhile, the Clouds and the Earth's Radiant Energy System (CERES; Wielicki et al. 1996) Surface Radiation Budget (SRB) team started to test the algorithm for possible global application. The CERES program is designed to provide crucial cloud and radiation measurements for studying cloud-radiation interaction. The space-borne CERES radiometer provides broadband total, shortwave (SW) and infrared window measurements at the top of atmosphere (TOA). Differencing the SW from the total measurements allows for a derivation of the longwave (LW) value. Deriving reliable estimates of SRB parameters is an important objective of the CERES project in order to provide complete picture of energy budget of the earth–atmosphere system. Since the SRB cannot be directly measured by satellite-borne instruments, the surface fluxes are derived with several different methods using combinations of radiation models, data assimilation products, and satellite measurements. The Surface and Atmospheric Radiation Budget (SARB; Charlock et al. 1997) component of CERES represents one such method where shortwave and longwave fluxes at the surface, at three levels in the atmosphere, and at the TOA are computed with a radiative transfer model. In addition to SARB, surface fluxes are being derived within CERES using two SW and two LW models, which are based on TOA-to-surface transfer algorithms or fast radiation parameterizations. These models are the Li et al. (1993) model (SW model A, clear sky only), the Darnell et al. (1992) model (SW model B), the Inamdar and Ramanathan (1997) model (LW model A, clear sky only), and the Gupta et al. (1992) model (LW model B). These models were incorporated into CERES products to provide independent sources of surface fluxes to compare with SARB results (Gupta et al. 2004). The Zhou-Cess algorithm represents a new methodology for deriving SDLW globally for both clear sky and cloudy sky using parameters readily available from satellite measurements. A vigorous test was performed using CERES Terra FM1 Ed2B single-scanner footprints and matched ground measurements from surface radiation measurement sites around the globe. Despite its simplicity, the algorithm performed very well for most of the geographical regions. Large biases were found for certain regions, most notably the Polar Regions where the atmosphere is extremely cold and dry. Systematic errors were also found for regions covered with ice cloud.

The current modifications of the algorithm are aimed to address the low water vapor and ice cloud situations to make the algorithm applicable

for global implementation in the CERES processing.

2. THE ORIGINAL MODEL BIAS

The Zhou-Cess (2001) algorithm took the form:

$$SDLW = a + b \bullet SULW + c \bullet ln(PWV) + d \bullet [ln(PWV)]^2 + e \bullet ln(1 + f \bullet LWP) \quad (1)$$

Where SULW is the surface upwelling longwave flux computed from the 2-meter air temperature using Stefan-Boltzmann's law assuming unity emissivity. PWV is the column precipitable water vapor and LWP is the cloud liquid water path in centimeter. The regression coefficients a, b c, d, e, f have values of 123.86, 0.444, 56.16, -3.65, 5.30, 1226.0, respectively. The algorithm was derived using observational data obtained from six Intensive Observation Periods (IOP) at the ARM SGP site and was verified with nine other SGP IOP datasets and TWP Manus data (Zhou and Cess 2001). The algorithm was not tested with observational data from other geophysical regions because of data availability problem.

2.1 The ARM NSA Data

Recent climate modeling and diagnostic studies indicate the Polar Regions are particularly sensitive to global climate change and important to mid-latitude climate and weather system. Radiation tends to dominate the Arctic heat budget in all seasons. Due to extreme weather conditions, the algorithms developed for mid-latitudes frequently do not work well for the Polar Regions. It is natural to test the Zhou-Cess algorithm when high quality observations from ARM North Slope of Alaska became available. The data used in the study was from January to December, 2000 from ARM Barrow facility. The Barrow facility is located at the northernmost point (71.32N, 156.61W) in the United States, 330 miles north of the Arctic Circle. The data were taken from the same instruments and processed the same manner as those used in Zhou-Cess (2001) for the SGP and TWP sites. The SDLW fluxes were pygeometer measurements and the surface upwelling fluxes were computed from the Surface Meteorological Observation Station (SMOS) 2-m surface air temperature. The column precipitable water and cloud liquid water were both measured by microwave radiometer (MWR). All data were averaged into half-hour products. The results show that the algorithm mostly underestimates the SDLW, with large negative bias at the low SDLW (Fig. 1). Further analysis found that 94% of the underestimated cases are related to very low water vapor amount (PWV < 0.81 cm). The low water vapor amount has resulted in very large negative value in the ln(PWV) term since the logarithmic function decreases very rapidly with decreasing water vapor below 1 cm. To remedy the problem, the ln(PWV) term was redefined to ln(1+PWV). This modification has the added advantage of producing very simple and reasonable relationships between SDLW and the water vapor terms PWV and LWP as the water vapor amounts asymptote toward zero.

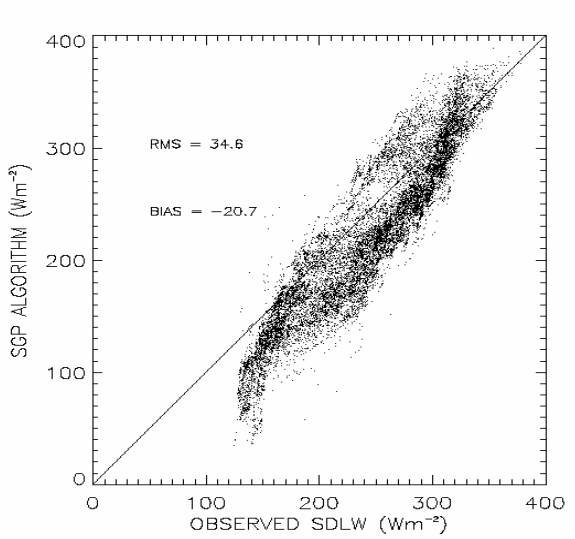

Fig. 1 Observed surface downwelling longwave flux versus calculated with original Zhou-Cess algorithm for data from Barrow, NSA from Jan.2000-Dec.2000.

Although Zhou-Cess (2001) conducted radiative transfer calculations for 6 default MODTRAN atmospheres (including subarctic summer and subarctic winter atmosphere) and their variations for providing basic relationships between SDLW and other parameters, the actual algorithm was derived using only observations at SGP site for illustrative purpose. For any nonlinear relationship, it is important that full range of data is adequately present in order to derive statistical relationship that applies to most situations. This is because the statistical relations (usually derived with least square fitting) will lean toward highly sampled situations and miss the under-sampled situations.

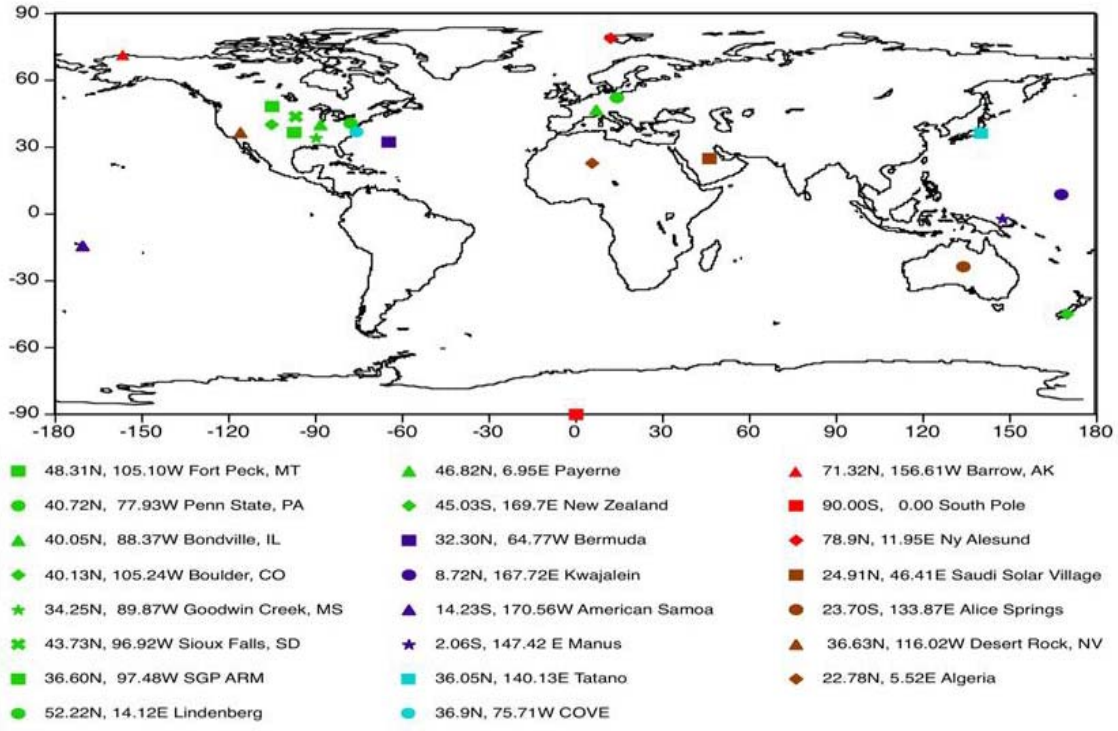

Fig. 3 Ground stations used in this study.

The importance of sampling can be illustrated in Fig.2 where a linear relationship is calculated for MODTRAN computed SDLW and SULW from Zhou and Cess (2001) (upper panel). Using upper portion (PWV>=0.5 cm) and lower portion (PWV < 0.5 cm) of the data gives very different slope and offset for a linear relationship. The log-square fit of PWV to the ratio of fluxes also depends significantly on different portion of sampling data (lower panel). The reason why the SGP algorithm does not produce good results for NSA data is because SGP data only represent middle range of the data (PWV) so that it won't apply to the low end of the curve.

Due to data availability, the original algorithm only used cloud liquid water path to account for cloud effect to the SDLW. For SGP and TWP site, since most of the ice clouds are high, their effect to SDLW is relatively small. It is not the case for the polar region, where most of the clouds are ice cloud and low in altitude, and the atmosphere water vapor is also very low. The effect of ice clouds on SDLW is not negligible.

2.2 Satellite Implementation

The CERES Single Scanner Footprint (SSF) product contains one hour of instantaneous CERES data for a single scanner instrument. The SSF combines instantaneous CERES data with scene information and cloud properties defined from a higher-resolution imager such as Visible/Infrared Scanner (VIRS) on TRMM or Moderate-Resolution Imaging Spectroradiometer (MODIS) on Terra and Aqua. The cloud properties

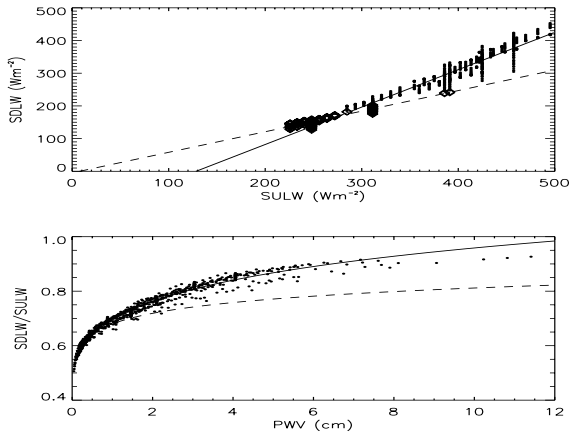

Fig. 2 Relationships between MODTRAN computed clear sky SDLW and SULW (upper panel) and flux ratio versus column water vapor (lower panel). The black and dot lines are linear regression fits (upper panel) and log-square fits (lower panel) using data points with PWV greater than 0.5 cm (solid line) and PWV less than 0.5 cm (dot lines), respectively.

are computed in the cloud subsystem of CERES processing (Minnis et al. 1997). All the input parameters for the Zhou-Cess algorithm are already computed or assembled in the current SSF processing.

The ground measurements are taken from CERES/ARM Validation Experiment (CAVE; Rutan et al. 2001) database (Fig. 3), which is maintained at NASA LaRC in a Web-accessible form for use in the CERES project and which is also available to the outside science community. Temporal matching of the satellite and site fluxes was done at the highest resolution of the site data.. Spatial matching was done to a distance of 20- km between the location of the site and the center of the CERES footprint. Values for all CERES footprints within the 20-km range of the sites and within the 1 minute interval were averaged together for comparison with the corresponding ground-based values (Gupta et al. 2004).

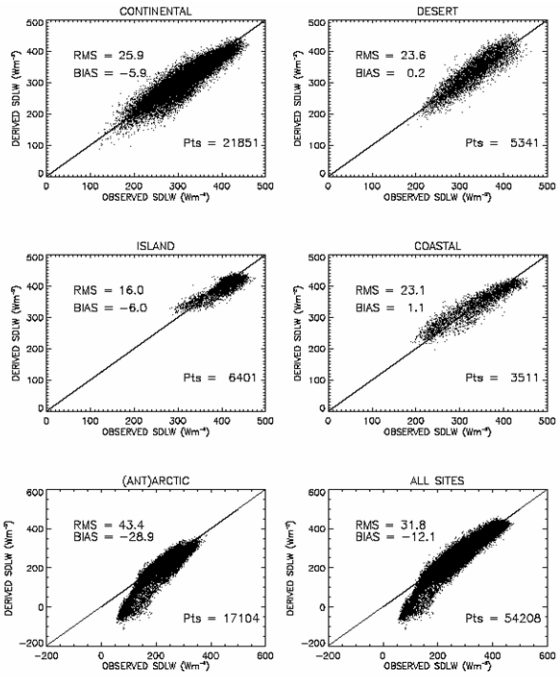

Fig. 4 Scatter plot of SDLW computed using original Zhou-Cess algorithm for Terra SSF Edition 2B versus ground measured SDLW for different scene types.

Fig. 4 shows the scatter plots of SDLW computed by original Zhou-Cess algorithm for Terra Edition 2B and collocated ground measurements. For most geographical regions (continental, desert, island and coastal area), the algorithm performs reasonably well, however it significantly underestimates SDLW in the Ant-arctic region when SDLW is below 200 Wm^{-2}. Most of the low values were observed at the South Pole where mean water vapor is only 0.34 cm. When the data is stratified with clear (Area_clr > 99.9%), water cloud (LWP > 5 g/m^2) and ice cloud (LWP < 5 g/m^2 and IWP> 1 g/m^2) cases, it was found that there is positive bias for most of the clear sky cases except in some Ant-artic cases (Fig. 5). Large negative bias was found for both water cloud and ice cloud, with ice cloud has even larger negative bias. The large negative bias for cloud sky flux might be due to lower cloud liquid water path generally observed from satellite than those observed from MWR in the SGP site. It was also found that some of the MWR measured cloud liquid water used in deriving the original algorithm might have been contaminated by rain or wetness from other forms of precipitation due to their unlikely larger value (LWP > 0.13 cm). The systematic difference between ice cloud and water cloud also indicates that ice clouds can play an important role for cases other than the warm, moist tropical cases. All these suggest that the algorithm should be re-derived using satellite observed cloud parameters and using more sites globally so that it would better represent various atmospheric conditions. In the revised algorithm, the effect of ice cloud will be considered by including ice water content the same manner as cloud liquid water but possibly less weight.

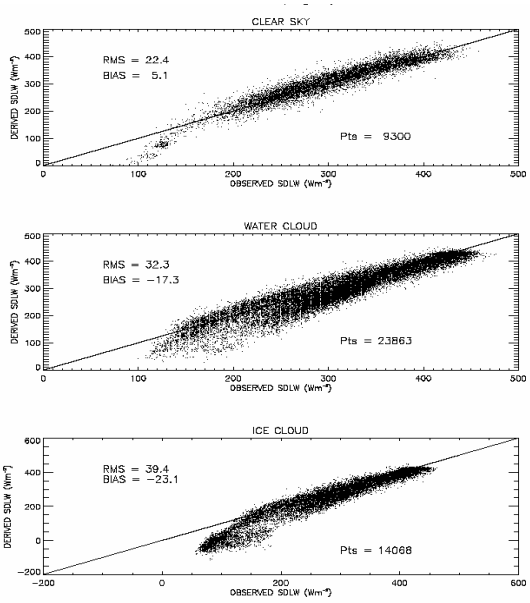

Fig. 5 Same as Fig. 3 but plotted for clear sky (Area_clr > 99.9%), water cloud (LWP>5 g/m^2) and ice cloud (LWP < 5 g/m^2, IWP>1 g/m^2) conditions.

3. REVISED ALGORITHM

Based on the above analysis, a new algorithm was derived which computes the fluxes for clear portion (F_{clr}) and cloudy portion ($_{Fcld)}$ of the sky separately and then sums the results for the all sky flux (F_{all}):

$$Fclr = a0 + a1 \cdot SULW + a2 \cdot ln(1 + PWV) + a3 \cdot [ln(1 + PWV)]^2 \quad (2)$$

$$Fcld = b0 + b1 \cdot SULW + b2 \cdot ln(1 + PWV) + b3 \cdot [ln(1 + PWV)]^2 + b4 \cdot ln(1 + LWP) + b5 \cdot ln(1+IWP) \quad (3)$$

$$Fall = Fclr \cdot Area\_clr \cdot 0.01 + Fcld \cdot (100 - Area\_clr) \cdot 0.01 \quad (4)$$

$$Fnet = SULW - Fall \quad (5)$$

a0 = 37.687, a1 = 0.474, a2 = 94.190,
a3 = -4.935
b0 = 60.349, b1 = 0.480, b2 = 127.956,
b3 = -29.794, b4= 1.626, b5 = 0.535

Where Area_clr and Area_cld are the percentage of clear and cloudy area in a single CERES footprint, respectively; SULW and PWV follow the same unit as in (1). LWP and IWP (in g/m^2) are not total for the pixel, but for the cloudy portion only as cloud fraction is explicitly taken into consideration. SULW is computed from surface temperature using unity emissivity. The surface air temperature and water vapor are from CERES meteorological data with the rest of parameters from CERES cloud analysis. In the above, clear sky is defined when Area_clr is greater than 99.9% and both LWP and IWP are set to zero.

The above regressions are derived using matched CERES observations and ground measured SDLW from 15 sites around the globe (Fig. 3) during 58 months from March 2000 to Dec 2004. There are 6028 clear sky cases (Area_clr > 99.9%) for deriving clear sky formula and 5788 overcast cases (Area_clr < 1%) data points to derive the cloud sky formula. These data consist of 43% of all collocated measurements during this period.

4. VALIDATION

The modified algorithm has been applied to the Terra Edition 2B and Aqua Edition 2A SSF data products. The Terra Edition 2B data, as mentioned above, spans from March 2000 to December 2004. Fig.6 shows scatter plots of SDLW of Terra Edition 2B computed with the modified Zhou-Cess algorithm versus ground measured SDLW over 29 sites around the globe stratified for different scene types. The modified algorithm has smaller bias (less than 1 Wm^{-2}) for most of the scene types except for the coastal area where systematic bias is 7.3 Wm^{-2}.

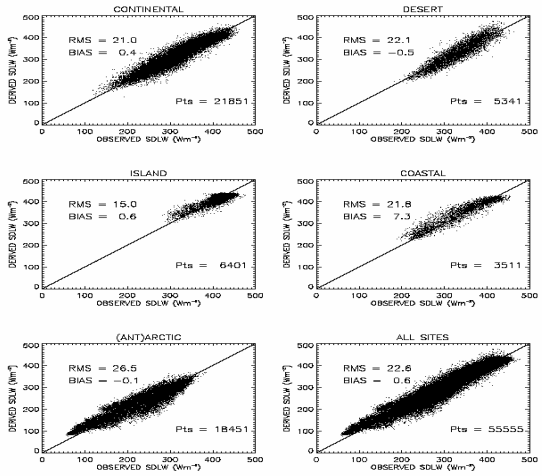

Fig. 6 Scatter plot of SDLW computed from modified Zhou-Cess algorithm versus ground measurements for different scene types for Terra Edition 2B product.

The modified algorithm has been applied to Aqua processing along with longwave LWA and LWB. The following results cover the period from July 2002 to March 2005 for Aqua 2A. The ground measurements are collected from the same 29 global sites as shown in Fig.3. All data available from these periods are used except for some data gaps. The validation was carried for clear sky and cloudy sky separately.

Table 1. Longwave clear sky flux computed from original LWC and modified LWC.

Sites # of Points	Original LWC Bias Wm^{-2}(%) σ Wm^{-2} (%)	Modified LWC Bias Wm^2(%) σ Wm^{-2} (%)
Continental 5012	6.71 (2.38) 20.9 (7.4)	-0.16 (-0.06) 16.6 (5.9)
Coastal 609	16.66 (5.84) 17.8 (6.3)	10.03 (3.52) 14.8 (5.2)
Ant-arctic 903	-137.00 (-121.96) 34.5 (30.7)	10.45 (9.30) 11.1 (9.9)
Desert 1640	-1.68 (-0.53) 24.4 (7.8)	-7.12 (-2.27) 23.9 (7.6)
Island 138	9.31 (2.47) 10.3 (2.7)	2.92 (0.77) 12.6 (3.3)
Global 8302	-9.81 (-3.61) 41.4 (15.3)	0.42 (0.15) 18.5 (6.8)

Table 2. Long wave clear sky flux computed from LWA, LWB and modified LWC.

Sites # of Points	LWA Bias Wm^{-2}(%) σ Wm^{-2} (%)	LWB Bias Wm^{-2}(%) σ Wm^{-2} (%)	LWC Bias Wm^{-2} (%) σ Wm^{-2} (%)
Continental 5012	-4.48 (-1.59) 15.8 (5.6)	-6.93 (-2.46) 15.4 (5.5)	-0.16 (-0.06) 16.6 (5.9)
Coastal 609	4.92 (1.72) 12.9 (4.5)	-0.15 (-0.05) 13.2 (4.6)	10.03 (3.52) 14.8 (5.2)
Ant-arctic 903	-16.02 (-14.30) 11.0 (9.9)	-8.83 (-7.88) 11.0 (9.9)	10.45 (9.30) 11.1 (9.9)
Desert 1640	-0.41 (-0.13) 22.8 (7.3)	-5.15 (-1.64) 21.1 (6.7)	-7.12 (-2.27) 23.9 (7.6)
Island 138	-0.75 (-0.20) 12.0 (3.2)	-0.77 (-0.20) 13.8 (3.6)	2.92 (0.77) 12.6 (3.3)
Global 8302	-4.18 (-1.54) 17.7 (6.5)	-6.19 (-2.28) 16.8 (6.2)	0.42 (0.15) 18.5 (6.8)

Table 1 compares the bias and random error of the original algorithm to those of the modified algorithm for clear sky flux. Using the modified algorithm reduces the huge negative bias for the Ant-arctic region from -137.0 Wm^{-2} to an acceptable -10.5 Wm^{-2}. The use of the modified algorithm has also improved either the bias or random error or both for most of the regions. The modified algorithm does produce biases for coastal and Ant-arctic) areas of order 10 Wm^{-2}, and globally, there is a <1 Wm^{-2} bias and a 18 Wm^{-2} standard deviation. Comparison of LWC with LWA and LWB for clear sky fluxes are shown in Table 2. The modified LWC has smaller bias for continental region than both LWA and LWB. It has larger systematic bias in the coastal and Desert area. The global mean bias is smaller for LWC probably due to cancellation of positive and negative bias. The random error of 18.5 Wm^{-2} is slightly higher than those of LWA (17. 7 Wm^{-2}) and LWB (16.8 Wm^{-2}).

Table 3. Long wave cloudy sky flux computed from original LWC and modified LWC.

Sites # of Points	Original LWC Bias Wm^{-2} (%) σ Wm^{-2} (%)	Modified LWC Bias Wm^{-2} (%) σ Wm^{-2} (%)
Continental 21117	-7.42 (-2.33) 28.0 (8.8)	0.61 (0.19) 22.6 (7.1)
Coastal 3302	1.80 (0.52) 21.2 (6.1)	6.00 (1.72) 18.5 (5.3)
Ant-arctic 17663	-46.63 (-20.17) 50.6 (21.9)	-0.89 (-0.39) 23.6 (10.2)
Desert 4170	8.19 (2.42) 28.1 (8.3)	9.67 (2.85) 27.7 (8.2)
Island 6729	0.58 (0.14) 13.5 (3.3)	0.95 (0.23) 12.5 (3.0)
Global 52981	-17.67 (-5.80) 40.1 (13.2)	1.20 (0.39) 23.6 (7.8)

Table 4. Long wave cloudy sky flux computed from LWB and modified LWC.

Sites # of Points	LWB Bias Wm^{-2} (%) σ Wm^{-2} (%)	LWC Bias Wm^{-2} (%) σ Wm^{-2} (%)
Continental 21117	-3.38 (-1.06) 22.4 (7.0)	0.61 (0.19) 22.6 (7.1)
Coastal 3302	2.51 (0.72) 19.0 (5.4)	6.00 (1.72) 18.5 (5.3)
Ant-arctic 17663	-6.17 (-2.67) 25.0 (10.8)	-0.89 (-0.39) 23.6 (10.2)
Desert 4170	11.88 (3.51) 28.8 (8.5)	9.67 (2.85) 27.7 (8.2)
Island 6729	5.71 (1.39) 14.8 (3.6)	0.95 (0.23) 12.5 (3.0)
Global 52981	-1.59 (-0.52) 24.4 (8.0)	1.20 (0.39) 23.6 (7.8)

Table 3 shows that the major improvement for cloudy sky flux also occurs at Ant-arctic region. The bias is reduced from -46.6 Wm^{-2} to -0.89 Wm^{-2}. There is also a modest improvement for the continental area. There is slightly larger bias for coastal and desert region. Globally, the bias is 1.2 Wm^{-2} and standard deviation 23.6 Wm^{-2}. Comparing LWC cloud sky flux with LWB, it is found that LWC performs slightly better in continental, Ant-arctic, desert and island regions, only slightly worse in coastal area (Table 4). When all sky fluxes are considered, the modified algorithm has improvement for most geographical regions in systematic error, except for slightly higher bias for coastal and island areas. The random error is reduced for every region (Table 5). The global mean bias of all sky fluxes is 1.1 Wm^{-2} and the standard deviation is 23.0 Wm^{-2}.

Table 5. Longwave all sky flux computed from original LWC and modified LWC.

Sites # of Points	Original LWC Bias Wm^{-2} (%) σ Wm^{-2} (%)	Modified LWC Bias Wm^{-2} (%) σ Wm^{-2} (%)
Continental 26129	-4.71 (-1.51) 27.2 (8.7)	0.46 (0.15) 21.6 (6.9)
Coastal 3911	4.12 (1.21) 20.9 (6.1)	6.63 (1.95) 18.1 (5.3)
Ant-arctic 18566	-51.03 (-22.64) 51.6 (22.9)	-0.34 (-0.15) 23.3 (10.3)
Desert 5810	5.40 (1.63) 27.5 (8.3)	4.93 (1.48) 27.4 (8.3)
Island 6867	0.76 (0.19) 13.5 (3.3)	0.99 (0.24) 12.5 (3.1)
Global 61283	-16.61 (-5.54) 41.1 (13.7)	1.09 (0.36) 23.0 (7.7)

5. CONCLUSIONS

An improved version of Zhou-Cess algorithm (2001) has been formulated which avoids the large errors in the SDLW at low water vapor conditions by adding an offset to the logarithmic water vapor term. The new algorithm also utilizes cloud fraction and cloud liquid and ice water paths available from the CERES SSF product to separately compute the clear and cloud portions of the flux. The new algorithm has been validated for the Terra Edition 2B and Aqua Edition 2A data against surface measurements at 29 stations around the globe. The results show significant improvement over the original version and are now comparable to more sophisticated algorithms currently implemented in the CERES processing. This revised version of Zhou-Cess algorithm will be incorporated into the CERES operational processing.

REFERENCES

Charlock, T. P., and Coauthors, 1997: Compute surface and atmospheric fluxes (system 5.0): CERES Algorithm Theoretical Basis Document Release 2.2), NASA/RP-1376, 84 pp. [Available online at asd-www.larc.nasa.gov/ATBD/ATBD.html.].

Darnell, W. L., W. F. Staylor, S. K. Gupta, N. A. Ritchey, and A. C. Wilber, 1992: Seasonal variation of surface radiation budget derived from ISCCP-C1 data. *J. Geophys. Res.,* **97**, 15741–15760.

Gupta, S. K., W. L. Darnell, and A. C. Wilber, 1992: A parameterization for longwave surface radiation from satellite data: Recent improvements. *J. Appl. Meteor.,* **31**, 1361–1367.

Gupta, S. K., D. P. Kratz, A. C. Wilber, and L. C. Nguyen, 2004: Validation of Parameterized Algorithms Used to Derive TRMM–CERES Surface Radiative Flux. *J. Atmos. Ocea. Tech.*, 21, 742–752.

Inamdar, A. K., and V. Ramanathan, 1997: On monitoring the atmospheric greenhouse effect from space. *Tellus.,* **49B**, 216–230.

Li, Z., H. G. Leighton, and R. D. Cess, 1993: Surface net solar radiation estimated from satellite measurements: Comparisons with tower observations. *J. Climate.,* **6**, 1764–1772.

Minnis, P., and Coauthors, 1997: Cloud optical property retrieval (system 4.3). CERES Algorithm Theoretical Basis Document (Release 2.2), NASA/RP-1376, 60 pp. [Available online at asd-www.larc.nasa.gov/ATBD/ATBD.html.].

Rutan, D. A., F. G. Rose, N. M. Smith, and T. P. Charlock, 2001: Validation data set for CERES Surface and Atmospheric Radiation Budget (SARB). *WCRP/GEWEX News,* Vol. 11, No. 1, International GEWEX Project Office, Silver Spring, MD, 11– 12. [Available online at www.gewex.org/feb01.pdf; data available online at www-cave.larc.nasa.gov/cave/.].

Stamnes, K., R. G. Ellingson, J. A. Curry, J. E. Walsh and B. D. Zak. 1999: Review of Science Issues, Deployment Strategy, and Status for the ARM North Slope of Alaska–Adjacent Arctic Ocean Climate Research Site. *J. Climat.*, 12, 46–63.

Stokes, G. M., and S. E. Schwartz, 1994: The Atmospheric Radiation Measurement (ARM) program: Programmatic background and design of the cloud and radiation testbed. *Bull. Amer. Meteor. Soc.,* **75**, 1201–1221.

Wielicki, B. A., B. R. Barkstrom, E. F. Harrison, R. B. Lee III, G. L. Smith, and J. E. Cooper, 1996: Clouds and the Earth's Radiant Energy System (CERES): An Earth Observing System experiment. *Bull. Amer. Meteor. Soc.,* **77**, 853–868.

Zhou, Y. P., and R. D. Cess, 2001:Algorithm development strategies for retrieving the downwelling longwave flux at the Earth's surface. J. Geophys. Res., 106, 12,477-12,488.